Journal of Microfluidic and Nanofluidic Research

Journal homepage: https://jmnr.sku.ac.ir

Research Article

Numerical Simulation of Newtonian Nanofluid Flow in an Expansion Channel

Amireh Nourbakhsh [a*], Amir Abbas Yaghoubi [b]

[a] *Department of Mechanical Engineering, Faculty of Engineering, Bu-Ali Sina University, Hamedan, Iran*

[b] *Department of Mechanical Engineering, Faculty of Engineering, Bu-Ali Sina University, Hamedan, Iran*

ARTICLE INFO

Article history:

Received: 2025-05-08

Revised: 2025-06-16

Accepted: 2025-06-18

Keywords:

Expansion channel;

Nnaofluid;

Vortex length;

Volume fraction.

ABSTRACT

This study investigates the behavior of Newtonian and nanofluid flows through a channel featuring a sudden expansion with an expansion ratio of 1:3, considering expansion angles of 30°, 45°, 60°, and 90°. Numerical simulations are conducted under laminar flow conditions using a two-dimensional incompressible flow model, incorporating nanofluids with nanoparticles (Al_2O_3, TiO_2, and CuO) dispersed in water at volume fractions of 0.5%, 0.75%, and 1%. The single-phase approach assumes thermal equilibrium between particles and fluid, reducing computational complexity. Key parameters, such as vortex length near channel walls, are examined in relation to Reynolds number, nanofluid type, nanoparticle concentration, and expansion angle. Results reveal that vortex length increases with Reynolds number, expansion angle, and nanoparticle volume fraction. Flow bifurcation and vortex asymmetry arise beyond critical Reynolds numbers, indicating flow instability. Validation against established data confirms the accuracy of the numerical model. These findings contribute to a better understanding of flow dynamics in sudden expansion geometries involving nanofluids, with implications for fluid transport and mixing applications.

1. Introduction

The flow of Newtonian fluids in sudden expansion geometries has been extensively studied, beginning with experimental investigations by Durst et al. [1], Cherdron et al. [2], and Ouwa et al. [3]. They analyzed flow downstream of a two-dimensional symmetrical sudden expansion, showing that the flow remains symmetrical at low Reynolds numbers, but when the Reynolds number exceeds 56, vortex asymmetry develops, producing rotational regions of differing sizes. This loss of symmetry in planar diverging flows results in vortices of varying lengths, a phenomenon called branching, which is evident when vortex length is plotted against Reynolds number.

Dagtekin and Unsal [4] expanded on these studies by investigating Newtonian fluid flow in sudden diverging transitions across a broad range of Reynolds numbers ($500 \leq Re \leq \infty$) and expansion ratios ($0.5 \leq ER \leq 5$). They examined vortex behavior in planar and axisymmetric configurations.

Scott and Mirza [5] studied laminar Newtonian flow in axisymmetric sudden expansions and, by solving the two-dimensional Navier-Stokes equations via the finite element method, demonstrated that vortex behavior in planar and

* **Corresponding author.**
E-mail address: *nourbakhsh@basu.ac.ir*

Cite this article as:

Nourbakhsh, A. and Yaghoubi, A.A., 2025. Numerical Simulation of Newtonian Nanofluid Flow in an Expansion Channel. *Journal of Microfluidic and Nanofluidic Research*, 2(2), pp. 108-113. https://doi.org/10.22034/jmnr.2025.15488.1016

axisymmetric expansions is similar and changes linearly with Reynolds number.

Oliveira [6] numerically examined viscoelastic fluid flow with constant viscosity using the FENE-CR model for a planar diverging expansion with a 1:3 conversion ratio, analyzing how concentration, extensibility, and Weissenberg number affect vortex length and streamline patterns, and produced bifurcation diagrams showing the effect of increasing Reynolds number on flow instability.

Oliveira et al. [7] investigated Newtonian fluid flow in symmetrical planar diverging channels with expansion ratios between 1.5 and 4 and Reynolds numbers from 0.5 to 200. They quantified vortex length and pressure drop, finding vortex length increases with Reynolds number at all expansion ratios. At low Reynolds numbers, increasing the expansion ratio reduces vortex length, whereas at higher Reynolds numbers, vortex length increases with expansion ratio.

Bettaglia et al. [8] explored the increase in vortex length at large expansion ratios, using the finite volume method to analyze how varying expansion ratios influence vortex lengths.

Shapira et al. [9] analyzed the linear stability of symmetric flow in sudden planar expansions, focusing on vortex-related phenomena. Durst et al. [10] conducted experimental and numerical studies of sudden expansions with a 1:2 expansion ratio to investigate vortex lengths and their variations.

Bell and Surana [11] studied the isothermal flow of a non-Newtonian power-law fluid in symmetrical sudden expansions (1:2 ratio) at a Reynolds number of 10, assessing how the power-law index influences vortex size and length. Fletcher et al. [12] examined how inlet velocity profiles affect flow characteristics in symmetrical sudden expansions.

Pinho et al. [13] showed that at low Reynolds numbers, velocity distributions near the expansion surface deviate slightly from the parabolic profile in sudden planar expansions. Hawa and Rosak investigated the influence of channel geometry asymmetry on flow behavior.

Layek et al. [14] studied steady Newtonian flow in axisymmetric converging channels with gradual expansions by finite difference methods, analyzing effects of Reynolds number and expansion height on wall shear stress, axial velocity, and pressure. They found that increasing expansion height or Reynolds number decreases maximum wall shear stress and observed that centerline velocity decreases less with increased Reynolds number or decreased expansion height.

The flow analyzed in this paper occurs in a channel with a sudden expansion and specific dimensions, with an expansion ratio of 1:3, a configuration widely studied in the literature. As shown in Fig. 1, the initial section of the channel is 1 meter long to ensure fully developed flow, while the final section extends to 3 meters. The diameter of the initial section is 10 cm, expansion is 30 cm in the final section. The expansion angles considered in this study are 30°, 45°, 60°, and 90°.

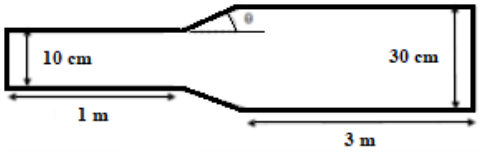

Fig. 1. Schematic of the channel with a sudden expansion.

2. Governing Equations

In this study, the flow geometry is two-dimensional with incompressible fluid flow, and the Reynolds number range corresponds to laminar flow. The main assumptions are:

1. The flow is two-dimensional, laminar, and steady.
2. The nanofluid behaves as a Newtonian, incompressible fluid.
3. Temperature is constant, so thermal effects on the flow are neglected.
4. The Reynolds number remains within the laminar regime.
5. Gravitational acceleration and body forces are neglected.

Four different fluids are analyzed: pure water and three nanofluids with nanoparticles dispersed in a water-based base fluid at volume fractions of 0.5%, 0.75%, and 1%. The problem is modeled using a single-phase approach, assuming the particle and fluid phases are in thermal equilibrium and share the same velocity. This approach reduces computational time significantly. To determine the nanofluid's thermophysical properties, appropriate empirical correlations are selected based on operating conditions and accuracy requirements. The viscosity μ_{nf} and density ρ_{nf} of the nanofluid are calculated from the properties of both the nanoparticles and the base fluid:

$$\mu_{nf} = \frac{\mu_f}{(1-\phi)^{2.5}} \quad (1)$$

$$\rho_{nf} = (1-\phi)\rho_f + \phi\rho_s \quad (2)$$

where ϕ represents the volume fraction of the solid nanoparticles in the nanofluid. The subscript *nf* denotes nanofluid, *f* indicates the base fluid, and *s* refers to the nanoparticles. The classical Brinkman model is used to calculate viscosity, while the density is obtained using the

correlation proposed by Pak and Cho [15]. Both models assume the nanoparticles are spherical in shape. At the channel inlet, a uniform velocity boundary condition is applied. For the outlet, a pressure outlet boundary condition is employed, assuming the fluid discharges into the environment, with the outlet gauge pressure set to zero. The channel walls enforce a no-slip boundary condition, meaning the fluid velocity at the walls equals the wall velocity. Since the walls are stationary, the fluid velocity at the channel walls is zero.

The governing equations include the mass conservation equation:

$$\frac{\partial \rho}{\partial t} + \frac{\partial \rho u}{\partial x} + \frac{\partial \rho v}{\partial y} = 0 \quad (3)$$

Momentum equation:

$$u\frac{\partial u}{\partial x} + v\frac{\partial u}{\partial y} = -\frac{1}{\rho}\frac{\partial p}{\partial x} + \frac{\mu}{\rho}\left(\frac{\partial^2 u}{\partial x^2} + \frac{\partial^2 u}{\partial y^2}\right) \quad (4)$$

$$u\frac{\partial v}{\partial x} + v\frac{\partial v}{\partial y} = -\frac{1}{\rho}\frac{\partial p}{\partial y} + \frac{\mu}{\rho}\left(\frac{\partial^2 v}{\partial x^2} + \frac{\partial^2 v}{\partial y^2}\right) \quad (5)$$

and energy equation:

$$u\frac{\partial T}{\partial x} + v\frac{\partial T}{\partial y} = \alpha\left(\frac{\partial^2 T}{\partial x^2} + \frac{\partial^2 T}{\partial y^2}\right) \quad (6)$$

Here, u and v are velocity components, p is pressure, μ is dynamic viscosity, T is temperature, and α is the expansion coefficient.

3. Grid Study

To obtain reliable results, the computational mesh must be carefully evaluated to ensure it can capture the flow characteristics accurately while enabling efficient data processing. To maximize the system's computational power and minimize unnecessary calculation time, a mesh convergence study is conducted. Initially, a coarse mesh is used, and one or more key quantities are monitored. The mesh density is progressively increased until the parameter of interest shows a negligible change compared to the previous refinement.

In this study, the parameter under investigation is the length of vortices formed near the upper and lower walls. This was evaluated at a 45° expansion angle, with pure water as the working fluid and a Reynolds number of 40. The results indicate that the difference between the third and fourth mesh refinements is minimal and does not significantly affect the solution (Table 1). However, the fourth mesh contains substantially more elements, leading to considerably higher computational time and cost. Therefore, the third mesh refinement is selected as the optimal mesh, and all subsequent calculations utilize this meshing.

Table 1. Grid independence test.

Grid	No. of elements	Dimensionless length of vortex
M1	17500	3.79
M2	31005	3.82
M3	69500	3.85
M4	277000	3.86

4. Validation

This section presents the validation of the numerical results. The expansion geometry with a 90-degree angle has been extensively studied by previous researchers. A key indicator for validating the solution is the dimensionless length of the vortices formed. Accordingly, the non-dimensional vortex length was calculated for an expansion ratio of 1:3 and a 90-degree expansion angle at various Reynolds numbers, and the results were compared with those reported by Oliveira [16]. As shown in Table 2, the differences between the numerical simulation results and Oliveira's data are minimal, demonstrating that the numerical model is sufficiently accurate and valid.

Table 2. Dimensionless vortex length obtained from the present results and those reported by Oliveira [16].

Re	Present work	Oliviera [64]	Error (%)
20	1.99	2.111	12
40	4.048	4.075	2.7
50	4.98	5.08	1

5. Results

This section presents the results from simulations conducted under various conditions, illustrated through contour plots and graphs. Vortex lengths were measured for expansion angles of 30°, 45°, 60°, and 90°, across Reynolds numbers ranging from 20 to 100, and for three types of nanofluids at three different volume fractions. The findings are summarized in graphs and tables for clarity.

5.1. Effect of nanofluid type

This section investigates the impact of nanofluid type on vortex length, considering a fixed expansion angle of 45° and a Reynolds number of 40. Vortex lengths were determined for four fluids: pure water and nanofluids containing 1% volume fractions of Al_2O_3, TiO_2, and CuO nanoparticles. As the channel cross-sectional area expands, the average flow velocity decreases while static pressure rises. The reduced velocity near the walls allows this pressure increase to overcome inertial forces, leading to flow separation and vortex formation adjacent to the channel wall. This abrupt pressure rise is illustrated in Fig. 2, which displays pressure variations along the centerline for water flow. According to Table 3, at this low

Reynolds number, vortices remain symmetrical in all cases. Changes in nanofluid properties, particularly density and inlet velocity, affect vortex length: higher nanoparticle density corresponds to longer vortices. The shortest vortices occur in pure water, while the longest are observed with the 1% CuO nanofluid.

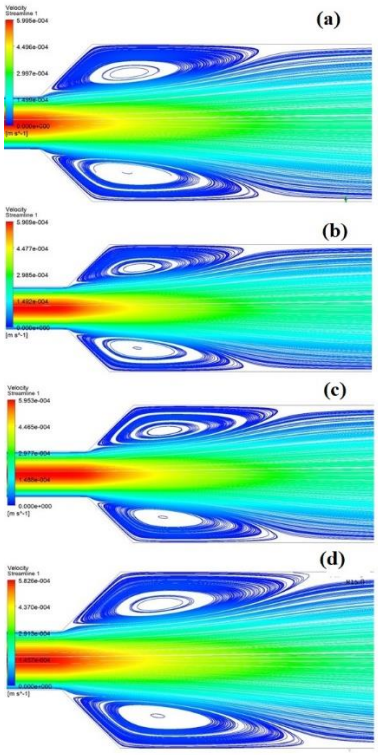

Fig. 2. Vortex length for (a) water, (b) Al_2O_3, (c) TiO_2, and (d) CuO, when Re = 40 and expansion angle is 45^0. The volume fraction for nanofluids is 1%.

Table 3. Dimensionless vortex length for different fluids.

Re	ϕ	Fluid	Dimensionless vortex length
40	-	Water	3.86
40	1%	Al_2O_3	3.93
40	1%	TiO_2	3.97
40	1%	CuO	4.021

5.2. Effect of Reynolds number

This section explores the influence of Reynolds number on vortex length for a specific nanofluid type. The flow is simulated at a 60° expansion angle using a 0.75% Al_2O_3 nanofluid, with results summarized in Table 4. At low Reynolds numbers, vortices near the upper and lower walls are symmetrical and equal in length, as shown by the streamlines in Fig. 3.

When the Reynolds number increases to the first critical value (Re = 75), the expansion-induced pressure rise overcomes viscous forces, disrupting the vortex symmetry and causing flow bifurcation. As depicted in Fig. 3, vortex symmetry is lost at this point. With further increases in Reynolds number, viscous forces weaken, and the flow can no longer sustain symmetrical vortex pairs. Beyond the second critical Reynolds number, the flow becomes more unstable, shifting toward one side of the channel, and a third vortex emerges near the upper wall, signaling increased flow instability. According to Fig. 3, this second critical Reynolds number is approximately 110.

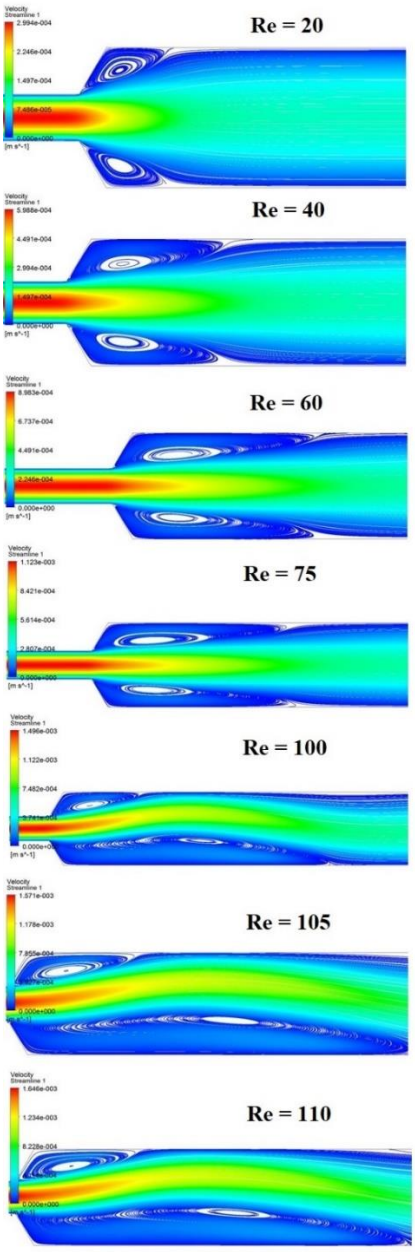

Fig. 3. Vortex length for Al_2O_3 and different Re values when the expansion angle is 45^0. The volume fraction for nanofluids is 0.75%.

Table 4. Dimensionless vortex length for different Reynolds numbers.

Re	Top vortex	Bottom vortex
20	1.9	1.9

40	3.71	3.71
60	5.69	5.69
75	6.94	6.94
100	3.71	11.31
105	3.78	11.83
110	3.83	12.08

5.3. Effect of expansion angle

To examine the effect of expansion angle on vortex length, the flow of a 1% volume fraction CuO nanofluid was simulated at a Reynolds number of 30 for expansion angles of 30°, 45°, 60°, and 90°. The results, presented in Table 5, show that vortex length increases with the expansion angle. The shortest vortices occur at a 30° angle, while the longest vortices form at 90°.

Table 5. Dimensionless vortex length for different expansion angles at Re = 30 for CuO with the volume fraction of 1%.

Expansion angle (^{0})	Dimensionless vortex length
30	1.135
45	2.88
60	2.93
90	3.08

5.4. Effect of nanofluid volume fraction

This section investigates the effect of nanofluid concentration on vortex length. Two types of nanofluids, CuO and TiO_2, were studied at volume fractions of 0.5%, 0.75%, and 1%, and compared with vortex lengths produced by the pure base fluid (water). The Reynolds number is kept constant at 45, and simulations were conducted at an expansion angle of 30°. The results, summarized in Table 6, indicate that the shortest vortex length and lowest instability occur with pure water. The addition of nanoparticles increases flow instability, which intensifies with higher nanoparticle concentrations, resulting in longer vortices. Thus, pure fluid exhibits the shortest vortices, while nanofluids at the highest concentration produce the longest.

Table 6. Dimensionless vortex length for different Reynolds numbers.

ϕ	Fluid	Dimensionless vortex length
-	Water	3.14
0.5%	TiO_2	3.20
0.75%	TiO_2	3.33
1%	TiO_2	3.48
0.5%	CuO	3.36
0.75%	CuO	3.53
1%	CuO	3.67

6. Conclusions

This paper has systematically analyzed the effects of flow parameters and nanofluid properties on vortex formation in a sudden expansion channel with a 1:3 expansion ratio. The numerical model was validated successfully through comparison with previous experimental and numerical studies. Results demonstrated that vortex length increases with Reynolds number, expansion angle, and nanoparticle concentration. At low Reynolds numbers, vortices remain symmetrical, but a transition to asymmetric flow and bifurcation occurs beyond critical Reynolds numbers, highlighting increased instability. Among nanofluids, those with higher nanoparticle volume fractions exhibited longer vortices due to enhanced density and altered flow characteristics. The single-phase modeling approach proved computationally efficient while capturing essential physics. Overall, this study provides valuable insights into the hydrodynamic behavior of Newtonian and nanofluid flows in sudden expansions, which can be applied in the design and optimization of fluid systems in engineering processes involving nanofluids.

References

[1] Durst, F., Melling, A., Whitelaw, J. H., 1974, Low Reynolds number flow over a plane symmetric sudden expansion, J. Fluid Mechanics, 64, pp. 111–128.

[2] Cherdron, W., Durst, F., Whitelaw, J.H., 1978, Asymmetric flows and instabilities in symmetric ducts with sudden expansions, J. Fluid Mechanics, 84, pp. 13– 31.

[3] Ouwa, Y., Watanabe, M., Asawo, H., 1981, Flow visualization of a two-dimensional water jet in a rectangular channel, Jpn. J. Appl. Phys, 20, pp. 243–247.

[4] Dagtekin, I., Unsal, M., 2011, Numerical analysis of axisymmetric and planar suden expansion flows for laminar regime, Int J Numer Meth Fluids, 65, pp.1133-1144.

[5] Scott, P.S., Mirza, F.A., 1986, A finite element analysis of laminar flows through planar and axisymmetric abrupt expansions, Computers & Fluids, 14(4), pp.423-432

[6] Oliveira, P.J., 2003, Asymmetric flows of viscoelastic fluids in symmetric planar expansion geometries, J Non-Newtonian Fluid Mechanics, 114, pp.33-63.

[7] Oliveira, P.J., Pinho, F.T., Schulte, A., 1998, A general correlation for the local loss coefficient in Newtonian axisymmetric

sudden expansions, Int J of Heat and Fluid Flow, 19, pp.655-660.

[8] Battaglia, F., Tavener, S.J., Kulkarni, A.K., Merkle, C.L., 1997, Bifurcation of low Reynolds number flows in symmetric channels, J AIAA, 35, pp.99-105.

[9] Shapira, M., Degani, D., Weihs, D., 1990, Stability and existence of multiple solutions for viscous flow in suddenly enlarged channels, Comp.Fluids, 18, pp.239-258.

[10] Durst, F., Pereira, J.C.F., Tropa, C., 1993, The plane symmetric sudden expansion flow at low Reynolds numbers, J Fluid Mech, 248(567).

[11] Bell, B.C., Surana, K.S., 1993, p-Version least squares finite element formulation for two-dimensional incompressible non-Newtonian isothermal and nonisothermal fluid flow, Int J Numer Methods Fluids, 18, pp.127–162.

[12] Fletcher, D.F., Maskell, S.J., Patrick, M.A., 1985, Heat and mass transfer computations for laminar flow in an axisymmetric sudden expansion, Comp Fluids, 13, pp.207–221.

[13] Pinho, F.T., Oliveira, P.J., Miranda, J.P., 2003, Pressure losses in the laminar flow of shear-thinning power-law fluids across a sudden axisymmetric expansion, Int J of Heat and Fluid Flow, 24, pp.747–761.

[14] Layek, G.C., Mukhopadhyay, S., 2008, Laminar flow separation in an axisymmetric sudden smooth expanded circular tube, J. Appl Math Comput. 28, pp. 235–247.

[15] Pak, B., Cho, I., 1998, Hydrodynamic and heat transfer study of dispersed fluids with sub-micron metallic oxide particles.", Exp.Heat transfer 11, pp. 151-170.

[16] Oliveira, P.J., 2003, Asymmetric flows of viscoelastic fluids in symmetric planar expansion geometries, J. Non-Newtonian Fluid Mech. 114, pp.33–63.